

THROUGH THE BASALTIC LOOKING GLASS: PAIRED REMOTE SENSING AND EXPERIMENTAL STUDIES OF GLASS ON MARS. K. M. Cannon¹, J. F. Mustard¹, R. F. Cooper¹, and S. W. Parman¹ ¹Department of Earth, Environmental and Planetary Sciences, Brown University, Providence RI 02906.
Email: kevin_cannon@brown.edu

Introduction: Glasses on Mars, formed by impact melting and volcanism, likely make up a significant fraction of the regolith because they accumulate over time and there have been few processes operating in the last ~3.5 Ga to destroy them [1]. These glasses have exciting astrobiological implications because they can host microbial colonies and preserve biosignatures [2-5]; they may have also served as precursor phases for observed alteration minerals [6,7], and they are important to consider for astronaut safety [8]. However, glass has not been widely detected on the surface with remote sensing studies [9]. Here we report on two related efforts: (1) detecting glasses at multiple spatial scales on Mars by modeling remotely sensed data and (2) enhancing these models with synthetic martian glasses.

Synthetic glasses: We are synthesizing four glass compositions relevant for the majority of volcanic and impact products on Mars (Fig. 1): (1) “ALK”: Alkaline basalt based on Curiosity measurements [10]; (2) “BLK”: Northwest Africa (NWA) 7034/7533, similar to the estimated bulk crustal composition [11,12]; (3) “VUL”: Adirondack-class basalt, believed to be representative of Noachian-Hesperian effusive volcanism [13]; (4) “OPS”: Representative of olivine-phyric shergottites, the most common martian meteorite type. We do not include high-Si glass (i.e., obsidian) or oth-

er terrestrial compositions because there is no evidence these are relevant for Mars.

All compositions are synthesized at five fO_2 conditions from QFM-2 to QFM+2 in 1-log unit steps, spanning the range of estimated martian conditions (reduced lavas to oxidized regolith). Varying fO_2 is important because it is known to shift Fe^{2+} crystal field absorption positions by hundreds of nanometers in lunar glass analogs [14], and its effects at mid-infrared wavelengths remain unexplored. All 20 glasses will be measured with: (1) Visible/near-infrared (VNIR) spectroscopy using the custom-built UV-VIS-NIR spectrometer at RELAB; (2) The Asteroid and Lunar Environment Chamber at RELAB to measure true emissivity; (3) Mössbauer spectroscopy to quantify Fe^{3+}/Fe^T ratios; (4) Electron probe microanalysis to verify major element compositions; (5) X-ray diffraction to ensure crystal-free glasses.

Remote sensing: The spectra from these synthetic glasses will feed into our spectral mixture models used previously to identify glass-rich proximal impactites on crater central peaks [15]. This will enhance the sensitivity of these models to identify glass by including glasses of multiple compositions with ranges in Fe^{3+}/Fe^T , instead of a single “glass” endmember that may not represent the glasses present on the surface.

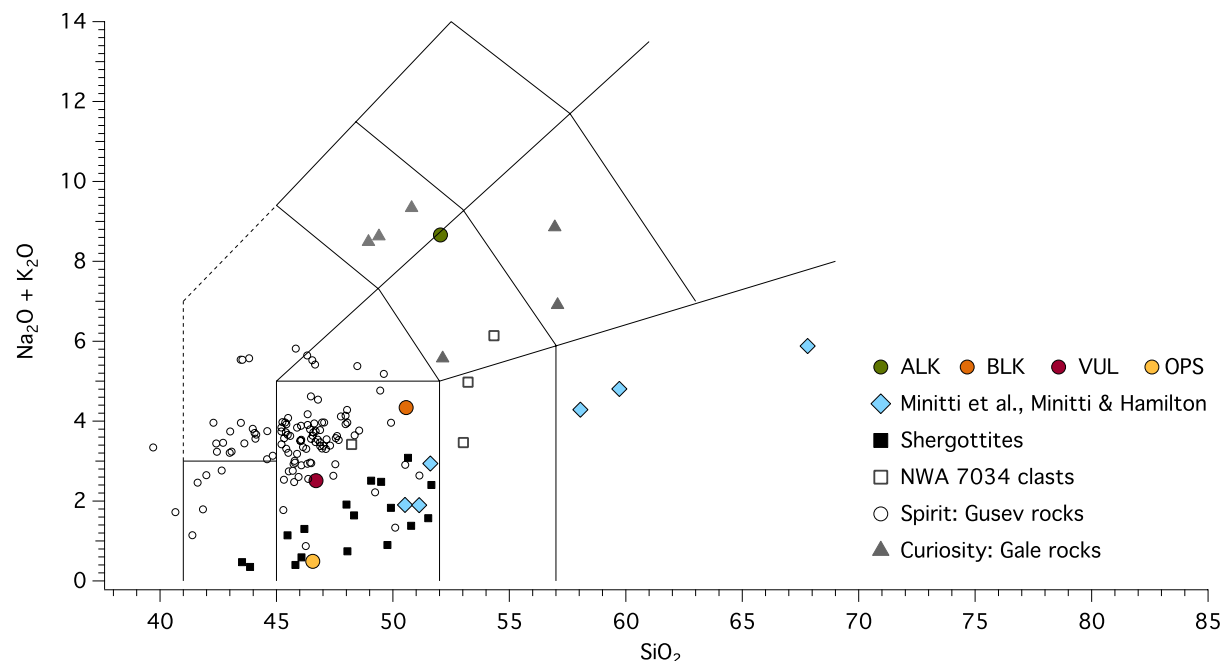


Figure 1. Total alkalis and silica diagram for Mars showing various datasets from rovers and meteorites. NWA 7034 clast data are from [20], and alkaline compositions in Gale are from [10]. Colored circles show our synthetic glasses, compared to previous synthetic Mars glasses (blue diamonds) [9,21].

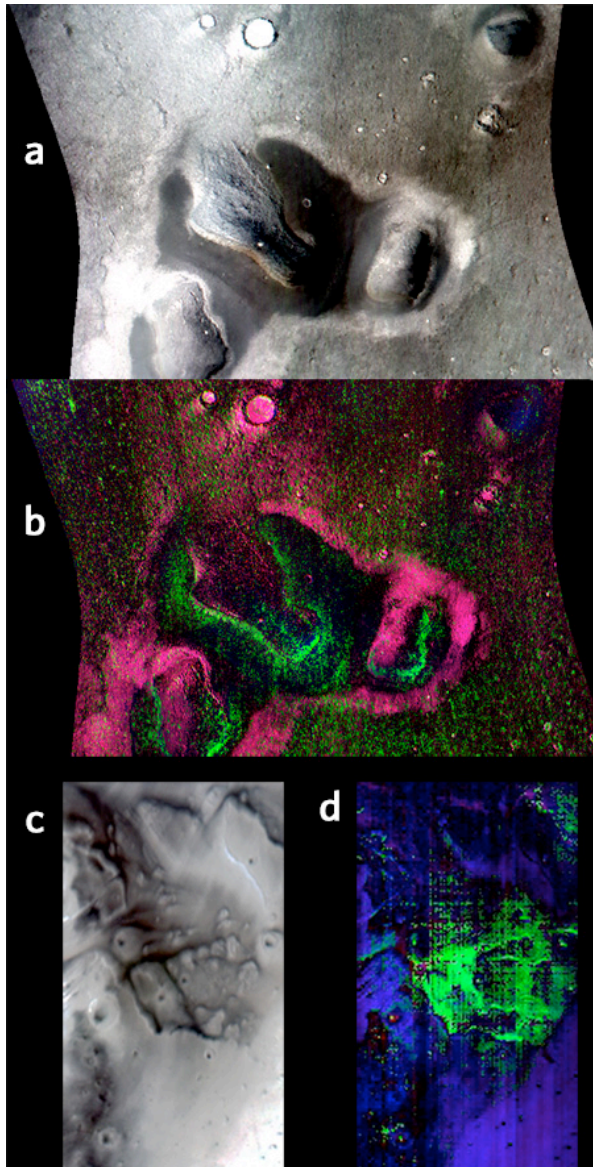


Figure 2. Examples of glass-rich exposures on Mars: a) CRISM scene FRT9A7D (width ~11 km) showing three probable cryptodomes [16] in Arcadia Planitia; b) modeled mineralogy [see 15] with red=olivine, green=glass and blue=pyroxene; c) OMEGA scene ORB0394_4 (width ~400 km) showing dark deposits in the mouth of Kasei Valles predicted to be part of a downrange strewnfield [19]; d) modeled mineralogy, with same colors as in (b).

As well, by substituting each of the synthetic glass spectra into our spectral library one at a time and performing F-tests relative to a glass-free library, we can determine which glass chemistries and oxidation states are best represented in different occurrences on the surface. We have expanded the scope of our previous

studies [15] to consider phreatomagmatic eruptions and possible ashfalls (CRISM scale), and distal ejecta deposits (OMEGA/TES scale).

Remote sensing results: We identify glass-rich deposits ranging from small-scale features to 100+km regions (Fig. 2).

Volcanic features: Farrand et al. [16] investigated spectral properties of volcanic cryptodomes in Arcadia and Utopia Planitiae, and found banding that could be caused by alternating glass-rich and glass-poor layers. We see evidence for this using our model, where there are distinct glass-rich halos surrounding the cryptodomes (Fig. 2a,b). We also see evidence for glass-rich deposits within the “mafic capping unit” prevalent in the Nili Fossae Region [17], hypothesized to be a possible ashfall (not shown).

Impact features: In addition to glass in probable impact melt/melt breccias draping central peaks [15], we find evidence for enhanced glass concentrations in large-scale low albedo deposits, hypothesized to be distal strewnfields [18,19]. Fig. 2c,d shows one such deposit at the mouth of Kasei Valles.

Conclusions and future work: Future work will fully characterize the synthetic glasses to make use of them in our spectral modeling. We will use true emissivity measurements of these glasses to better address glass abundances in the regolith as a whole, making use of TES data and quantitative abundance modeling.

References: [1] Cannon K. M. and Mustard J. F. (2014) *LPSC XLV*, Abstract #1962. [2] Schultz P. H. et al. (2014) *Geology*, 42, 515. [3] Sapers H. M. (2015) *EPSL*, 430, 95. [4] Howard K. T. et al. (2013) *Nat. Geosci.*, 6, 1018. [5] Sapers H. M. et al. (2014) *Geology*, 42, 471. [6] Peretyazhko T. S. et al. (2015) *GCA*, 173, 37. [7] Newsom H. E. (1980) *Icarus*, 44, 207. [8] Liu Y. et al. (2008) *J. Aero. Eng.*, 21, 272. [9] Minitti M. E. and Hamilton V. E. (2010) *Icarus*, 210, 135. [10] Sautter V. et al. (2015) *Nature Geosci.*, 8, 605. [11] Agee C. B. et al. (2013) *Science*, 339, 780. [12] Humayun M. et al. (2013) *Nature*, 503, 513. [13] Monders A. G. et al. (2010) *MAPS*, 42, 131. [14] Bell P. M. et al. (1976) *LPSC VII*, 2543. [15] Cannon K. M. and Mustard J. F. (2015) *Geology*, 43, 635. [16] Farrand W. H. et al. (2011) *Icarus*, 211, 139. [17] Edwards C. S. and Ehlmann B. L. (2015) *Geology*, 43, 863. [18] Wrobel K. E. and Schultz P. H. (2007) *Seventh Int. Conf. Mars*, Abstract #3093. [19] Schultz P. H. and Mustard J. F. (2004) *JGR*, 109, E01001. [20] Santos A. R. et al. (2015) *GCA*, 157, 56. [21] Minitti M. E. et al. (2002) *JGR*, 107, E5, 5030.